CHAPTER II

THEORY AND LITERATURE REVIEWS

THEORY

2.1 Organic solar cells

2.1.1 Background

With limitation of process technology, manufacturing cost and environmental friendliness of the production of the inorganic solar cells, the organic solar cells have become highly interesting alternatives for solar energy conversion. The first generation of organic photovoltaic solar cells is based on a single organic layer sandwiched between two metal electrodes of different work functions [12, 13]. The second generation is the bilayer heterojunction (p-n type semiconductor) [14]. Later on, an organic tandem cell was developed. It is a three layer p-i-n like structure with a co-deposited interlayer between the p-type (hole conducting) and n-type (electron conducting) layers [15]. In recent years, polymer conjugation was developed as a single layer device with slightly low power conversion efficiencies. The addition of the C_{60} derivatives to the conjugated polymers [16-18] led to the development of polymer–fullerene bilayer heterojunction [19] and bulk heterojunction devices [20, 21].

2.1.2 Dye sensitized solar cell

The production technology of this kind of the solar cells offers low cost and simple manufacture. Currently, many researches reported nearly 10% AM1.5 efficiency for dye-sensitized solar cells (DSSCs) [22]. The dye-sensitized solar cells are

composed of a conducting glass substrate, a porous semiconductor layer coated with an absorbed sensitizing dye, a redox electrolyte and metal electrode [23].

2.1.2.1 Operating principles of dye-sensitized solar cell

The dye-sensitized solar cells produce electric current by the following five steps [24] **(Figure 2.1)**.

i. The photons (light) are absorbed by dye molecules and initiate photo excitation of electrons.

ii. Electrons from the dye molecules move to the semiconductor, TiO_2, causing the oxidation of the dyes.

iii. The extracted charge can consequently perform electrical work in an external circuit.

iv. The oxidized species in the electrolyte are regenerated at the counter electrode.

v. The circuit is completed by reducing the oxidized dye with electron moving from the electrolyte or a hole-conductor.

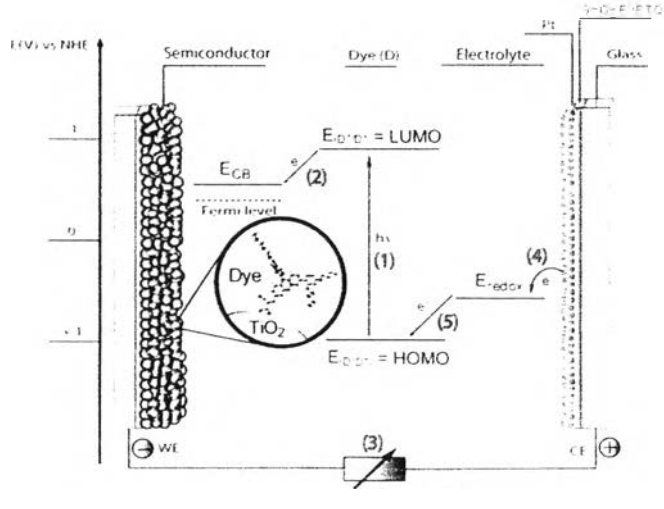

Figure 2.1 Operation of the dye-sensitized solar cell

2.1.2.2 Criterion for designing of organic photosensitizers

The promising photosensitizers should have the following properties [24]:

- Broad absorption band in the visible region and toward the near- IR region
- High absorption coefficient
- Efficient electronic communication with the electrode
- Environment friendly.
- High stability under the working condition
- Proper physical properties for the production process

2.1.3 Bulk heterojunction solar cells

Bulk herterojunction solar cell is an organic solar cell with mix donor and acceptor molecules in active layer. Normally, bulk heterojunction solar cell consists of transparent substrate, electrodes, one of which has to be transparent, a hole transport layer (HTL), an electron transport layer (ETL) and an active layer [25] as shown in **Figure 2.2.**

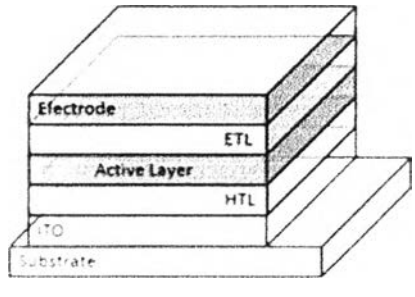

Figure 2.2 Schematic setup of the bulk heterojunction solar cell

The active layer contains a mixture of an electron donating conjugated polymers or conjugated pigments (p-type material) and an electron acceptor (n-type

material) some of the popular p- and n- materials [25] are shown in **Figure** 2.3(a) and 2.3(b), respectively.

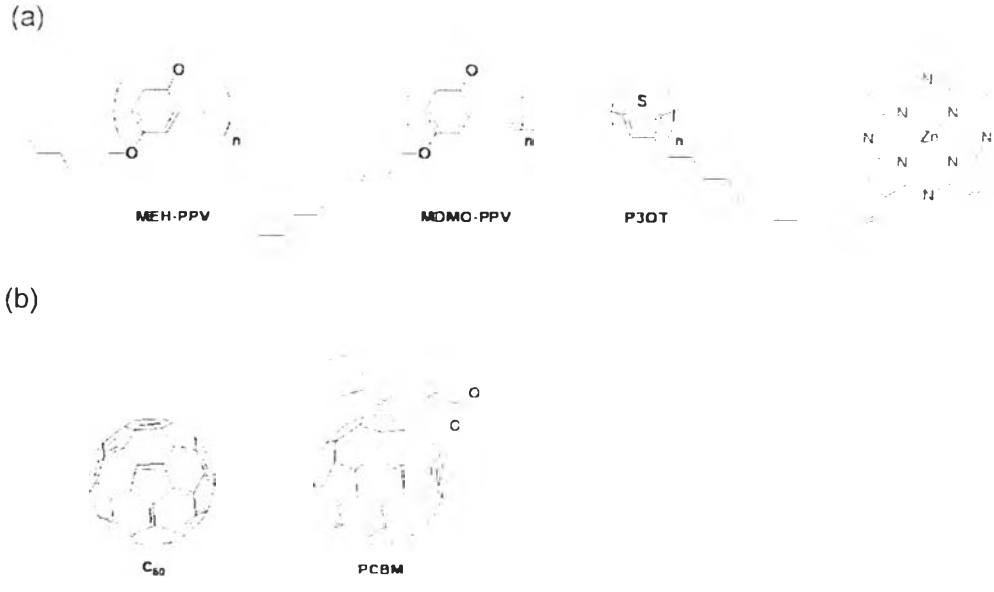

Figure 2.3 Examples for (a) donor and (b) acceptor materials used in the bulk heterojunction solar cells

2.1.3.1 Operating principles of the bulk heterojunction solar cells

The bulk heterojunction solar cells produce electric current by the following steps which can be described by **Figure 2.4**. [26]

Step 1. Light absorption

The sunlight passes through a transparent electrode to an active layer. Donor and acceptor in the active layer absorb photons, encouraging electrons movement from highest occupied molecular orbital (HOMO) to lowest unoccupied molecular orbital (LUMO) of the dye.

Step 2. Exciton diffusion

Excitons diffuse to donor/acceptor interface where the excitons dissociate into free carriers.

Step 3. Exciton dissociation (charge transfer)

Exciton dissociation is generated by the electrochemical potential different between the LUMO of the donor and the LUMO of the acceptor.

Step 4. Charge collection

The dissociated electrons and holes move to electrode. Electrons are collected at the cathode and hole are collected at the anode.

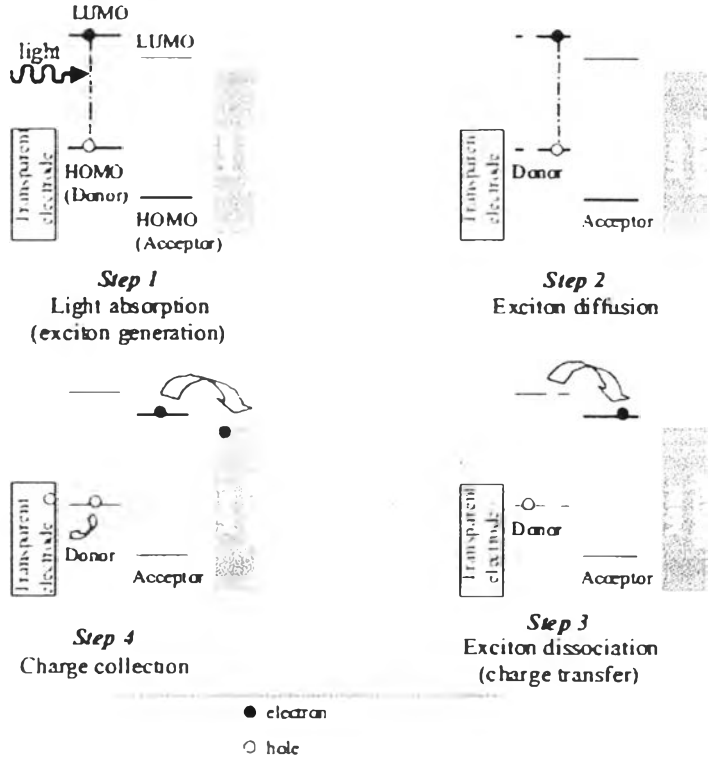

Figure 2.4 The simplified four basic steps of photocurrent generation in the bulk heterojuction solar cell

2.1.3.2 Desirable properties of the active layer

The promising active layer should have the following properties [26] :

i. Donor and acceptor materials in the active layer show exhibit broad absorptionbands to near-infrared region with high absorption coefficient.

ii. Electronic energy levels of the donor and acceptor exhibit low bandgap (LBG) materials. The LUMO and the HOMO of the donor is higher than those of the acceptor for efficient charge transfer.

2.2 Ligand to Metal and Metal to Ligand Charge Transfer

Molecular orbital of a ligands consists of $\sigma, \sigma^*, \pi, \pi^*$ and nonbonding (n) orbitals. Charge transfer occurs when the ligand molecular orbitals are full. Charge transfer is a result of the electronic movement from generated from the ligand molecular orbital to the empty or partially filled metal d-orbitals. The absorption that arise from ligand-to-metal charge-transfer (LMCT) process [27] (**Figure 2.5**).

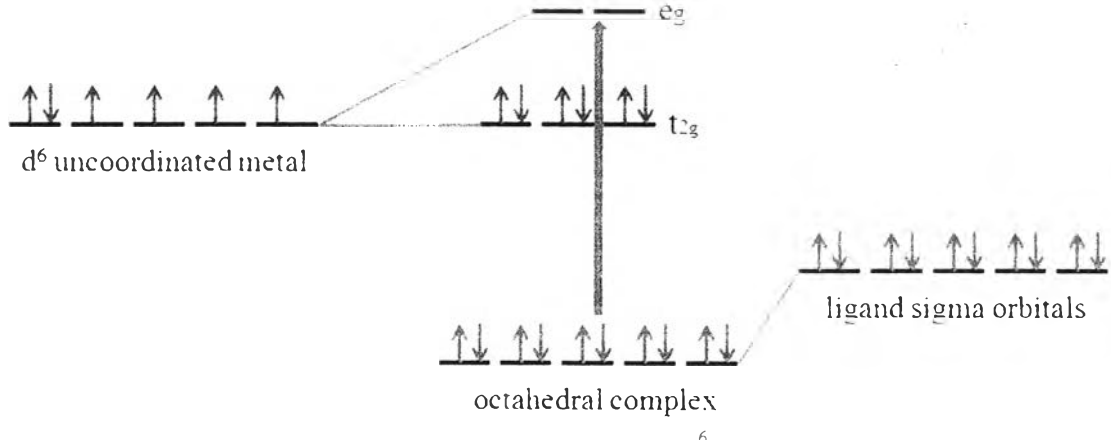

Figure 2.5 The LMCT process involving an octahedral d^6 complex

The LMCT transitions result in intense band, on the other hand the forbidden d-d transitions give rise to weak absorptions. LMCT appear in the reduction of the metal. Metal-to-ligand charge transfer (MLCT) [27] (**Figure 2.6**) may happen with a low oxidation state metal (electron rich) and the ligand possesses low-lying empty orbitals (for example CO or CN^-). The MLCT transitions result in intense band, on the other hand the forbidden d – d transitions give rise to weak absorptions. MLCT appear in the oxidation of the metal.

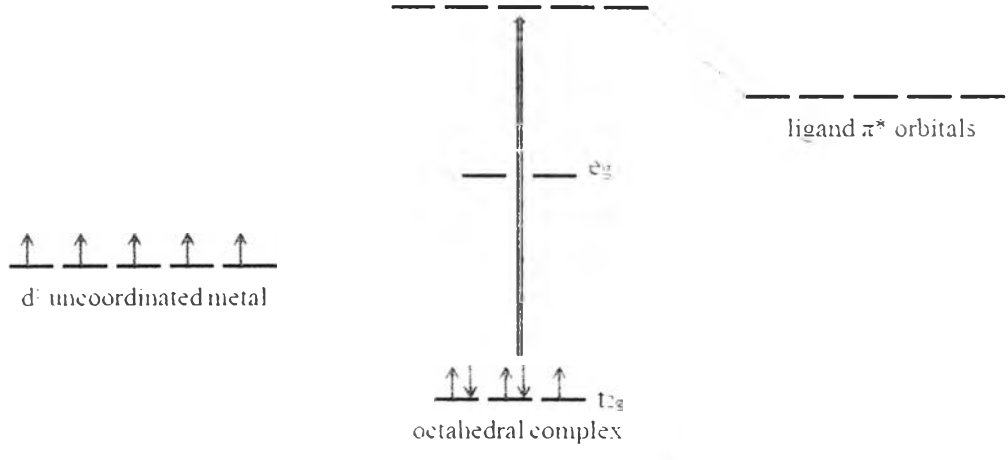

Figure 2.6 The MLCT process involving an octahedral d^5 complex.

2.3 Literature reviews

In 2000, Yu *et al.* [28] reported a synthesis of two series of polyamide and polyester derivatives based on 2,2′-bipyridine-5,5′-dicarboxylic acid. These polymers formed a complex with Ruthenium *via* the 2,2′-bipyridine moiety as shown in **Figure 2.7**. The polymeric ruthenium complex showed red emission resulted from the emission from the MLCT of the ruthenium complexes. The process was described to be an energy transfer from the polymer backbone chain to the metal complex parts.

Electroluminescent (EL) devices based on some polymers exhibited potential to be used as a light-emitting material with high thermal stability.

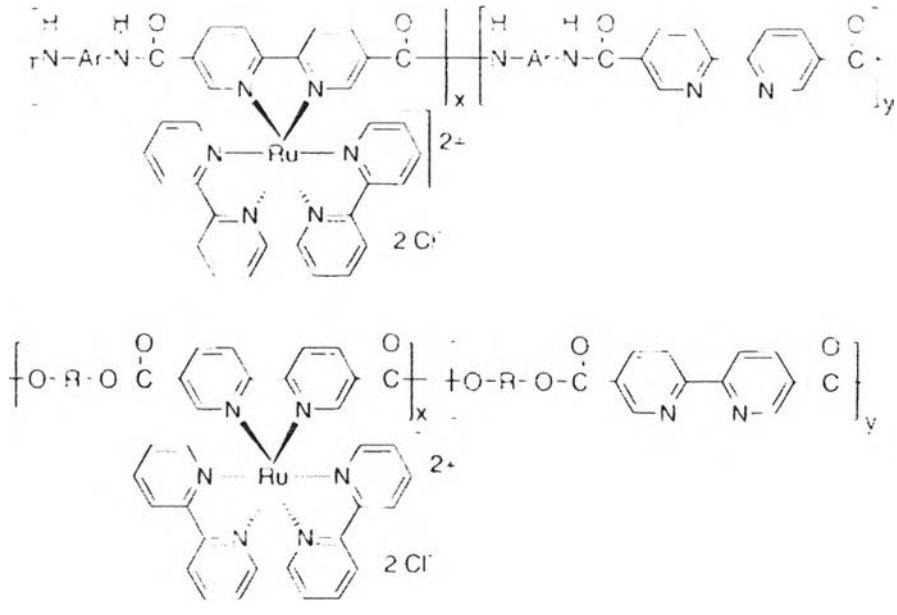

Figure 2.7 Polyamide ruthenium complexes (top) and polyester ruthenium complexes (bottom)

In 2005, Zong and Thummel [11] reported a synthesis of a new family of Ru(III) complex catalysts for water oxidation. The complexes were treated directly with an excessive amount of a 4-substituted pyridine to afford the complexes as shown in **Figure 2.8**. The complexed showed broad UV-Vis absorption in the red region.

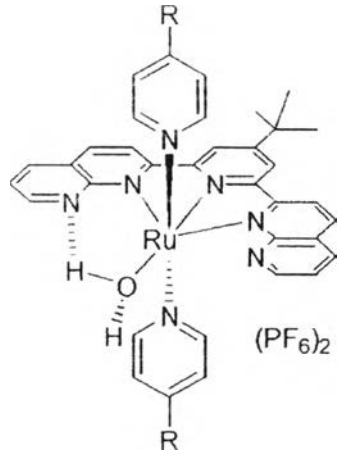

R = NMe_2, CH_3 and CF_3

Figure 2.8 Ru complexes synthesized by R. Zong and P. Thummel

In 2005, Kaizumi, Tanaka [10] reported a 2,6-bis(2-naphthyridine)pyridine (bnp) and its Ru complex as shown in **Figure 2.9**. The UV-Vis absorption spectra of these complexes showed absorption maxima at 525 and 526 nm respectively.

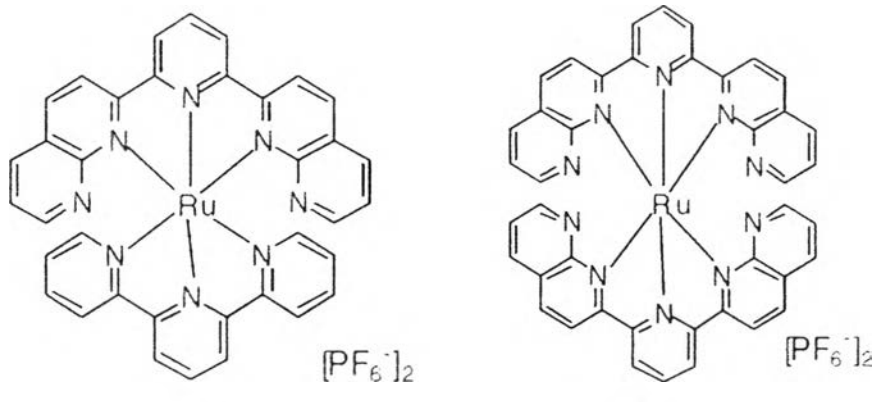

Figure 2.9 The structures of (a) $[Ru(bnp)(tpy)(PF_6)_2$ and (b) $[Ru(bnp)_2](PF_6)_2$

In 2006, Kukrek *et al.* [6] reported a synthesis of a 2-(pyrid-2'-yl)-1,8-naphthyridines having a carboethoxy or carboxylic group attached at the 4- and 4'-positions. The complexes of these ligands with Ru(II) and NaNCS were also described (**Figure 2.10**). The absorption band of these complexes extended to the red region

DSSCs based on these dyes exhibited incident photon-to-current efficiencies in the region beyond 625 nm which were considerably greater than the prototype N3 dye.

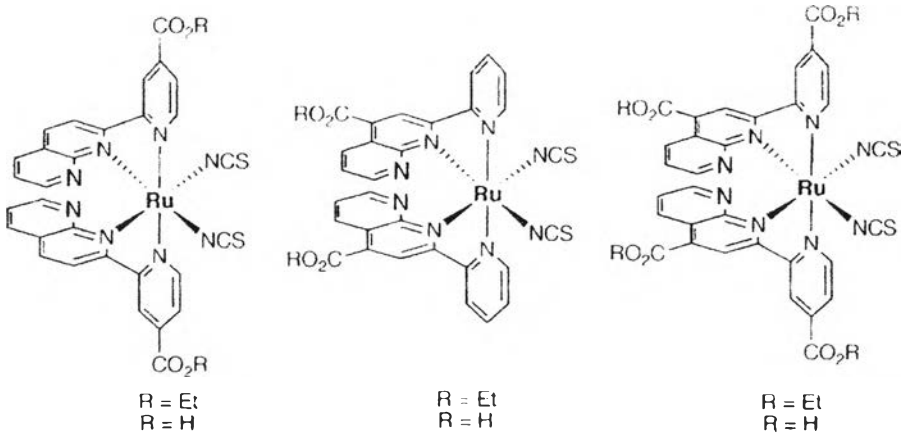

Figure 2.10 Ru(II) and NaNCS complexes of 2-(pyrid-2′-yl)-1,8-naphthyridines ligands